The International Journal of Advanced Manufacturing Technology (2019) 101:501–509
https://doi.org/10.1007/s00170-018-2918-5

ORIGINAL ARTICLE

Two-dimensional thermal error compensation modeling for worktable of CNC machine tools

Xinyuan Wei[1] · Enming Miao[2] · Hui Liu[1] · Shanlin Liu[1] · Suxin Chen[3]

Received: 31 May 2018 / Accepted: 22 October 2018 / Published online: 3 November 2018

Abstract

The conventional thermal error compensation for computer numerical control machine tools in ISO 230-3:2007 is based on a single positioned point on a worktable; this guideline ignores the thermal error differences of different locations across an entire worktable. As a result, a reduced compensation effect is achieved for the whole worktable, although the single-point compensation model generally provides high prediction accuracy. The 2D thermal error compensation method, which can greatly improve the compensation effect of the worktable, is proposed in this study. This method builds a 2D thermal error map model parallel to the worktable at each time point. The thermal error at any position on the workbench can be predicted accurately. Thus, this compensation method can significantly reduce the influence of thermal error differences on the compensation effect across the whole worktable. The thermal error prediction results and compensated experimental results show that the compensation effect of this new method is better than that of the conventional single-point method for the whole worktable.

Keywords CNC machine worktable · 2D thermal error map model · Least squares surface modeling

1 Introduction

During the process of operating a computer numerical control (CNC) machine, multiple heat sources exist, and the temperature field is complex because of the effects of spindle rotation, cutting parameters, and environment temperature. As a result, the relative position between the tool and workpiece changes, leading to processing errors for the machine [1, 2]. Temperature-induced changes in the relative position serve as an important basis for evaluating the thermal errors of CNC machine tools [3]. Statistics reveal that thermal errors account for 40–70% of the total machining errors of such tools [4, 5].

Electronic supplementary material The online version of this article (https://doi.org/10.1007/s00170-018-2918-5) contains supplementary material, which is available to authorized users.

✉ Enming Miao
miaoem@163.com

[1] School of Instrument Science and Opto-electronics Engineering, Hefei University of Technology, Hefei 230009, China

[2] School of Mechanical Engineering, Chongqing University of Technology, Chongqing 400054, China

[3] School of Mechanical Engineering, Hefei University of Technology, Hefei 230009, China

The software thermal error compensation technique, which predicts thermal error values with the thermal error compensation model, is a highly effective and economical means to improve the accuracy of machine tools [6, 7].

Recently, researchers worldwide have characterized the thermal properties of many CNC machine tools by the thermal deformation of the spindle at a single positioned point of worktable in relation to ISO 230-3:2007 [8]. Substantial research has focused on the selection of modeling algorithms and modeling temperature variables [9–15]. In particular, Abdulshahed et al. [9] used a thermal imaging camera to measure the temperature (in the context of the thermal error) of spindle Z, screened temperature-sensitive points through the gray relational model and fuzzy clustering algorithm, and then combined these strategies with an adaptive neural fuzzy inference system to establish a thermal error model. Miao et al. [11, 12] studied the changes in the characteristics of temperature-sensitive points in a machine tool spindle through annual tracking experiments. Liu et al. and the author [13] subsequently modeled and compensated for the thermal deformation of a positioned point through a multiple linear regression model, and this approach has been effectively applied in engineering practice.

However, in the machining process, the workpiece possesses a certain volume shape, which occupies a certain space

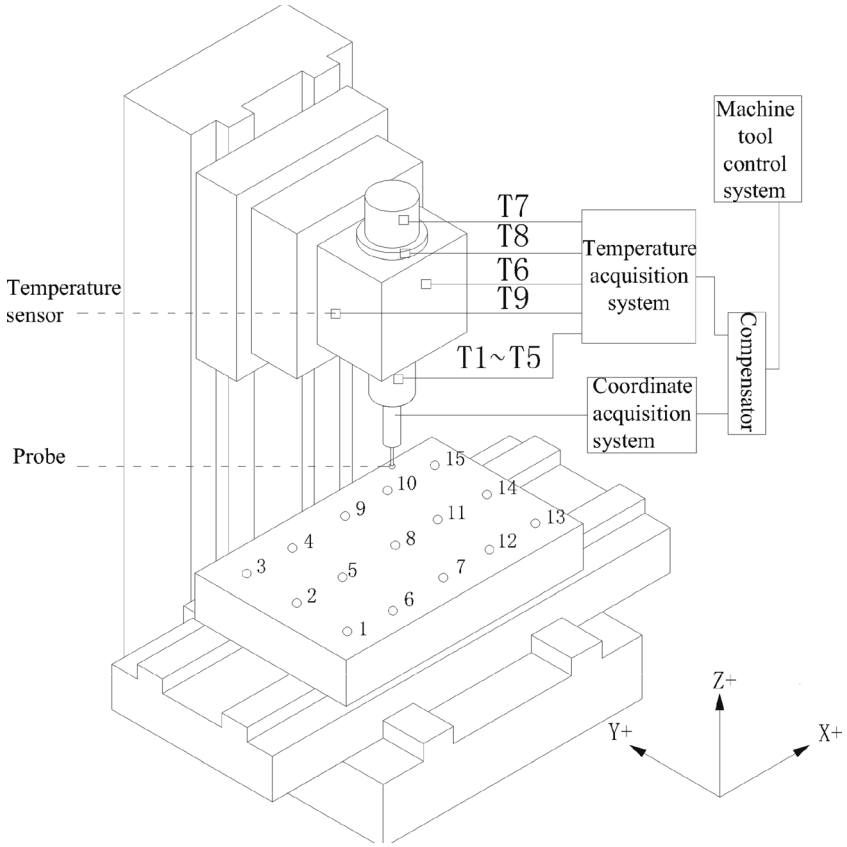

Fig. 1 Schematic of the placement distribution of the temperature sensors and the 15 positions across the worktable. T1–T9 refer to the temperature sensor numbers (sensor T10, which is placed in the machine casing, is not labeled because the machine casing is not shown); 1–15 are the numbers of the 15 measuring positions on the worktable

area of the worktable instead of a single positioned point. The worktable is also connected to a guide rail through a slider; this connection allows the worktable to undergo dynamic and complex thermal deformation [16, 17]. The tool's displacement/orientation is significantly different depending on the location in the workspace [18]. Consequently, a large uncertainty is introduced in the thermal error compensation for the whole worktable if only a single point on the worktable is used to establish the compensation model. To date, few researchers have focused on thermal compensation for the whole worktable. In 2015, Zhang et al. [17] proposed a multilocation forecasting model with the piecewise fitting compensation method to improve the compensation effect of a large worktable. In 2016, S. Ibaraki et al. [18] introduced a new method for measuring 2D motion trajectory thermal deformations that reduces the measurement time substantially.

In the present study, a 2D thermal error map method is proposed for the thermal error compensation of a whole worktable. First, 15 positions on the worktable are selected to measure the thermal errors of the whole worktable in the X, Y, and Z directions. The temperature changes of key parts of the machine tool are also measured at the same time point. Second, the differences in thermal error at different positions on the worktable are analyzed, and the thermal error models of 15 positions in each direction are established. On the basis of the thermal error prediction values of 15 positions, the 2D thermal error map model of the whole worktable at that time point is built using the least squares surface fitting algorithm [19]. Then, the prediction results of the 2D error map models are compared with those of the conventional positioned single-point model. Finally, the 2D thermal error map compensation method and single-point method are separately

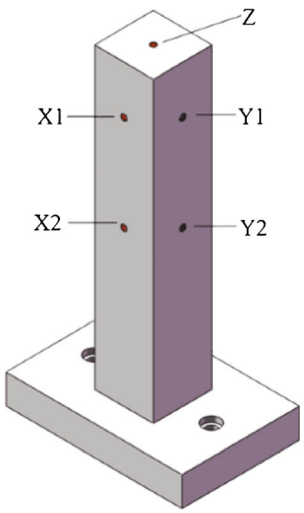

Fig. 2 Diagram of the standard measurement part

Table 1 Installation locations and functions of temperature sensors

Sensors	Installation site	Function
T1, T2, T3, T4, T5	Front bearing of the spindle	Spindle temperature measurement
T6, T9	Spindle box	Spindle temperature measurement
T7, T8	Spindle motor	Spindle motor temperature measurement
T10	Machine frame	Ambient temperature measurement

embedded into the compensator of the CNC machine tool to compensate for the thermal error in real time with the use of the external coordinate origin offset function [20] of the CNC machine.

2 Measurement experiments of the thermal error in three directions across the whole worktable

2.1 Experimental scheme

To measure the thermal errors in the X, Y, and Z directions across the whole range of the worktable, we select 15 positions spread out evenly on the worktable and mount one target block at each position. As shown in Fig. 1, these 15 positions, labeled 1 to 15, are selected in accordance with the worktable size and experimental time. The target block is shown in Fig. 2, in which points X1, X2 are used to measure the X-direction thermal error; points Y1, Y2 are used to measure the Y-direction thermal error; and point Z is used to measure the Z-direction thermal error. During the tests, the thermal error in each direction is calculated by the deviation of the coordinate values of the corresponding points. The coordinate value of each point is measured by an online detection system probe.

Ten temperature sensors (Fig. 1) are used to measure the temperature changes of the key parts of the machine simultaneously. The functions of the temperature sensors are listed in Table 1. According to the international standard ISO 230-3:2007 [8], the spindle idles at a constant speed, whereas the table travels at a constant feed rate along the X- and Y-axes during each experiment. The temperature and thermal errors are acquired every 5 min; each experiment lasts for 4 h. A total of seven batches of experiments are carried out, as listed in Table 2, and are recorded as K1–K7. The K1 experiment is used for modeling, whereas the K2–K7 experiments are adopted to verify the prediction accuracy of the model.

2.2 Experimental configuration

A typical C-type CNC vertical machining center (Leaderway-V450) is used as the research object. The size of the worktable is 620 mm × 350 mm. The measurement system is composed of a temperature measurement system and a coordinate acquisition system. Ten temperature sensors DS18B20 (measurement accuracy of 0.2 °C, highest resolution of 0.0625 °C) are used to collect the temperature values. The coordinate acquisition system is composed of an online testing system (including probe and IR receiver), an expansion I/O unit of the machine tool, a coordinate acquisition card, and a computer (Fig. 3).

3 Building of 2D thermal error compensation models for the whole worktable

The thermal errors in the X, Y, and Z directions of the K1 experimental data are analyzed. The analysis results indicate that the thermal errors between different positions across the whole worktable differ from one another. Thus, compensation models of 2D thermal error maps for the whole worktable are necessary. Fuzzy clustering with a gray correlation degree algorithm is used to select the temperature-sensitive variables for modeling. The multiple linear regression algorithm is used to establish the single-point thermal error models for all three

Table 2 Experimental parameters

Batch	Spindle speed (rpm)	Feed rate (mm/min)	Time (idle/measure)	Ambient temperature (°C)
K1	6000	1500	5 min/1 min	26.12–30.75 °C
K2	6000	1500	5 min/1 min	26.12–30.75 °C
K3	6000	1500	5 min/1 min	26.75–30.37 °C
K4	6000	1500	5 min/1 min	27.87–32.31 °C
K5	6000	1500	5 min/1 min	29.87–32.75 °C
K6	6000	1500	5 min/1 min	29.87–33 °C
K7	6000	1500	5 min/1 min	26.81–31.31 °C

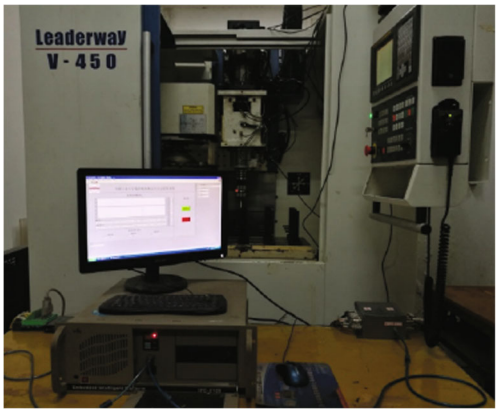

Fig. 3 Experimental device

directions of the 15 positions. The 2D error map model at each time point is then established by using the least squares surface fitting algorithm [19] on the basis of the prediction values of 15 single-point models at the same time point. The 2D thermal error map models in three directions for the whole worktable at all times are finally obtained.

3.1 Analysis of thermal errors in three directions of the whole worktable

According to the experimental data of K1, the trends of the thermal errors of the 15 positions in the X, Y, and Z directions are obtained. The trends of thermal errors in the X direction of point X1 and point X2 are separately plotted in Fig. 4(a1) and (a2), respectively. Similarly, the trends in the Y direction of Y1 and Y2 are separately plotted in Fig. 4(b1) and (b2), respectively. The trends in the Z direction are plotted in Fig. 4(c). The measurement results of X2, Y2, and Z are studied in this paper.

The temperature variation curves of the 10 temperature sensors are also plotted in Fig. 5. Three time points, namely,

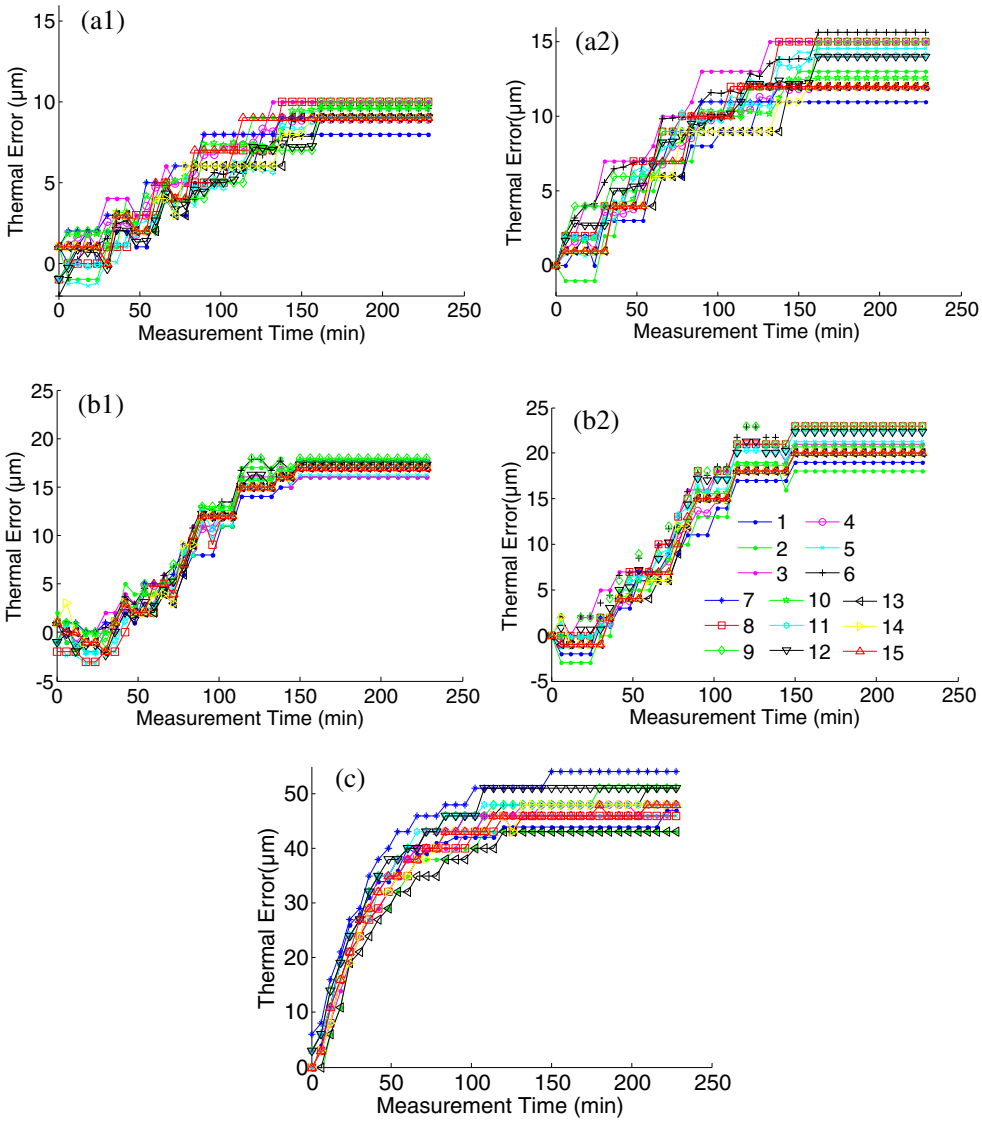

Fig. 4 Thermal errors in the X, Y, and Z directions of K1. 1–15 mark the 15 positions on the worktable

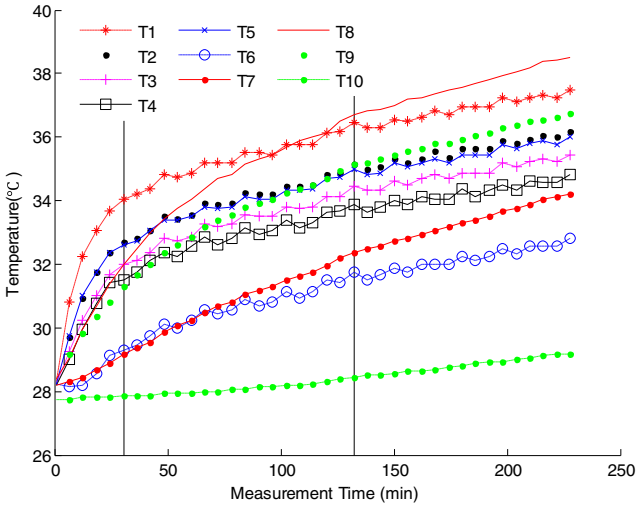

Fig. 5 Trends of temperature change. T1–T10 mark the 10 temperature sensors. The vertical black lines are the chosen measurement time points

the 0th, 30th, and 132nd minute, are selected to analyze the thermal errors of the whole worktable. The 2D thermal error maps of the whole worktable at these time points in each direction are separately drawn using the surf function in MATLAB and the cubic spline interpolation surface method [21, 22] (Fig. 6(a), (b), and (c)).

Figure 6(a), (b), and (c) shows significant differences in thermal errors in the whole range of the worktable in all directions. The maximum values of the thermal error differences at the same time point reach 5 μm in the X and Y directions and 11 μm in the Z direction. However, the thermal errors of different positions on the whole worktable are assumed to be the same in the conventional single-point method. This finding directly affects the compensation effect over the whole range of the worktable. Therefore, 2D thermal error map models must be established to achieve a high compensation precision for the whole worktable.

3.2 Building of single-point thermal error models for 15 positions

In this study, the multiple linear regression algorithm is adopted to build single-point thermal error models of the 15 positions. In the model, the finite temperature-sensitive points are the independent variables, and the thermal deformation is the dependent variable.

Table 3 Results of temperature-sensitive point selection

Directions	X	Y	Z
Results	T7, T10	T8, T10	T1, T8

In the modeling process, the use of excessively few temperature variables reduces the prediction accuracy because of information loss, whereas the use of an excessively high number of temperature variables increases the complexity of the model and results in collinear errors [11]. Therefore, the temperature variables should be selected before modeling. As described in reference [11], the method combining fuzzy clustering and gray correlation degree is used to select the temperature variables. The selection results are listed in Table 3.

In accordance with the temperature-sensitive point selection listed in Table 3, a binary linear regression model is built for each position on the worktable in each direction. The general expression of the model is as follows:

$$\Delta r_{p,t} = b_{p,0} + b_{p,1}\Delta T_{m,t} + b_{p,2}\Delta T_{l,t} + e_t \quad (1)$$

In Eq. (1), $\Delta r_{p,\ t}$ represents the tth thermal error in one direction of the pth position on the worktable, where $p = 1, 2, \cdots, 15$. $\Delta T_{m,\ t}$ and $\Delta T_{l,\ t}$ represent the tth temperature value changes of the two temperature-sensitive points T_m and T_l. e_t is the deviation of the prediction value from the actual measured value, also known as the residuals. ($b_{p,\ 0}, b_{p,\ 1}, b_{p,\ 2}$) are the estimates of the regression coefficients of corresponding temperature variables, which can be calculated by:

$$\begin{pmatrix} b_{p,0} \\ b_{p,1} \\ b_{p,2} \end{pmatrix} = \left(\Delta T_C{}^T \Delta T_C\right)^{-1} \Delta T_C{}^T \times \Delta R_p \quad (2)$$

where $\Delta T_C = (C, \Delta T_m, \Delta T_n)$ and ΔT_m and ΔT_l are the measurement data of T_m and T_l, respectively. $\Delta T_m = \{0, \Delta t_{m,\ 2}, \ldots, \Delta t_{m,\ n}\}^T$, $\Delta T_l = \{0, \Delta t_{l,\ 2}, \ldots, \Delta t_{l,\ n}\}^T$, $C = \{1, \ldots, 1\}^T$, $\Delta R_p = \{\Delta r_{p,\ 1}, \ldots \Delta r_{p,\ n}\}^T$, and n is the number of measurement data points in K1.

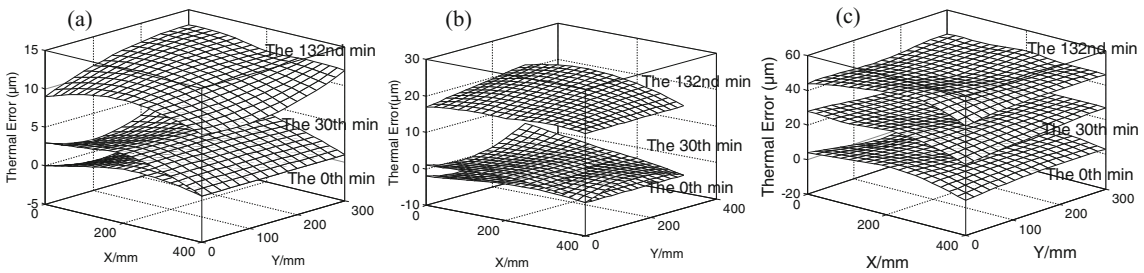

Fig. 6 Thermal error map in the (a) X, (b) Y, and (c) Z directions in the 0th, 30th, and 132nd minute

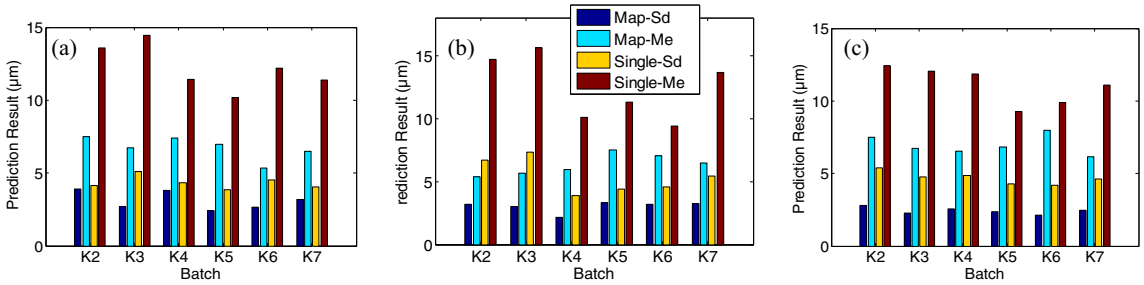

Fig. 7 Prediction results of the (a) X, (b) Y, and (c) Z directions. "Map-Sd" and "Map-Me" represent the Sd and Me, respectively, of the 2D error map models, whereas "Single-Sd" and "Single-Me" represent the Sd and Me, respectively, of the conventional single-point model. Among these models, $S_d = S_i/n$, and $M_e = M_i/n$ ($i = 1, 2, \cdots, n$). Si and Mi are the prediction residual standard deviation and maximum residual error at each time point, respectively

As indicated by the above modeling method, 15 single-point multiple linear regression thermal error models in the X, Y, and Z directions can be established on the basis of the experimental data of K1.

3.3 Building of 2D thermal error map compensation models for the whole worktable

The thermal error prediction values of the 15 positions at each time point are calculated in accordance with the 15 single-point models built in Section 3.2. Then, the 2D thermal error map model of the whole worktable at each time point is obtained by using the least squares fitting algorithm [16]. The 2D map model built in this study is a binary cubic polynomial model, expressed as follows:

$$\begin{aligned}\Delta r_t = {} & a_{0,t} + a_{1,t}x + a_{2,t}y + a_{3,t}x^2 + a_{4,t}xy + a_{5,t}y^2 \\ & + a_{6,t}x^3 + a_{7,t}x^2y + a_{8,t}xy^2 + a_{9,t}y^3\end{aligned} \tag{3}$$

In Eq. (3), ($a_{0,t}, a_{1,t}, \cdots a_{9,t}$) are estimates of coefficients for corresponding variables, x and y are the values of the (X, Y) coordinate of the machine tool, and Δr_t is the tth thermal error compensation value of the position with (x, y) coordinates on the worktable in one direction. $a_{0,t}, a_{1,t}, \cdots a_{9,t}$ can be obtained by solving:

$$\begin{pmatrix} a_{0,t} \\ \cdots \\ a_{9,t} \end{pmatrix} = \left(M^T M\right)^{-1} M^T \times N \tag{4}$$

where $M = (K, X, Y, X^2, XY, Y^2, X^3, X^2Y, XY^2, Y^3)$, $K = \{1, \ldots, 1\}^T$, $X = \{x_1, \ldots, x_{15}\}^T$, $Y = \{y_1, \ldots, y_{15}\}^T$ (the other is the same), $N = \{\Delta r_{1,t}, \ldots \Delta r_{15,t}\}^T$, and x_p and y_p are the coordinates of the 15 positions.

For example, the 2D thermal error map model in the Z direction in the 30th minute is obtained as follows. The temperature increments in the 30th minute are read on the basis of the experimental data, where $\Delta T_{16} = 2.68^{\circ}$C and $\Delta T_{86} = 0.63^{\circ}$C. The thermal error prediction values in the Z direction of the 15 positions are calculated. As a result, the 2D thermal error map model in the 30th minute can be built in accordance with Eq. (3) as follows:

$$\begin{aligned}\Delta z_{30}(x,y) = {} & 9.3580 \\ & + \begin{pmatrix} 727.22x - 2.2339x^2 - 1.8440xy - 2.5055y^2 \\ -0.0003x^3 + 0.0113x^2y - 0.00098xy^2 + 0.0139y^3 \end{pmatrix} \times 10^{-4}\end{aligned}$$

The standard deviation of the fitting of this model is S_0 = 0.35 μm.

The 2D thermal error map models of the whole worktable at any time point can be established by the above calculation method. The temperature values are varied; thus, the 2D thermal error map models are dynamic and involve real-time equations. This result holds great flexibility and predictive ability in engineering applications. Accurate and real-time thermal error compensation for the whole worktable is realized, with the 2D thermal error map compensation method embedded into the compensator of CNC machine tools. This strategy greatly improves the compensation effect over that of the conventional fixed single-point compensation method.

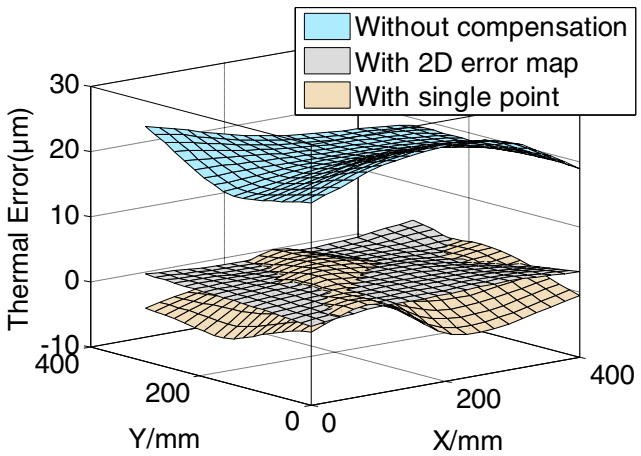

Fig. 8 Thermal error map of the whole worktable in the Z direction before and after compensation at the 30th minute of K2

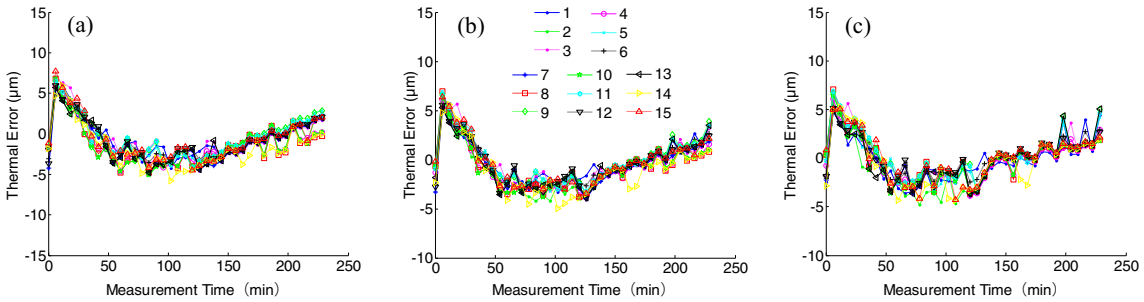

Fig. 9 Thermal errors in the (a) X, (b) Y, and (c) Z directions of 15 points by the 2D error map method

4 Accuracy analysis and implementation of 2D thermal error map compensation models

4.1 Comparison of the prediction results

The thermal errors of 15 positions in experiments K2–K7 are predicted from the 2D error map models and the single-point model separately built by K1. The residual standard deviation (Sd) and the maximum residual errors (Me) are taken as the prediction results. The single-point model is presented in Section 3.2, that is, the intermediate position of the worktable (position no. 8).

The prediction results of two compensation methods are presented as bar graphs in different directions (Fig. 7(a)–(c)).

In Fig. 7, the prediction results predicted by 2D error map models, including Sd and Me, are smaller than those predicted by the single-point model in all directions. Sd is decreased by 1.21 μm (27.9% of the single-point model) in the X direction, by 2.37 μm (44.0% of the single-point model) in the Y direction, and by 2.26 μm (48.0% of the single-point model) in the Z direction. Me is reduced by 5.46 μm (44.8%) in the X direction, by 6.10 (49.0%) in the Y direction, and by 4.14 μm (37.3%) in the Z direction.

The thermal errors without compensation and the prediction residual errors predicted by the two compensation methods of the whole worktable in the Z direction in the 30th minute of the K2 experiment are shown in Fig. 8.

The thermal error in the whole range of the worktable is sharply reduced after compensation. The thermal error map of the worktable with the 2D error map method is closer to the zero plane than the result of the single-point method. Thus, the 2D error map method is more effective than the single-point method over the whole range of the worktable.

4.2 Implementation of thermal error compensation

The 2D thermal error map method is first embedded into the compensator of the Leaderway-V450 CNC machine tool. Then, the temperature values of the temperature-sensitive points and the coordinate value of the machine tool acquired in real time are used to calculate the thermal error compensation value at this position. Finally, the value is inputted into the CNC system, and the compensation is realized through the external coordinate origin offset function [20] of the system.

The thermal errors of the 15 positions in the X, Y, and Z directions under the 2D thermal error map compensation method are measured, and the measurement results are shown in Fig. 9(a), (b), and (c), respectively. Similarly, the thermal errors obtained using the single-point compensation method are presented in Fig. 10(a), (b), and (c). Accordingly, the actual compensation effect of the 2D thermal compensation method is compared with that of the single-point method.

Figure 9(a), (b), and (c) shows that the maximum differences of the thermal errors over the whole range of the worktable at the same time point are 3.81, 3.37, and 4.52 μm in the X, Y, and Z directions, respectively. Figure 10(a), (b), and (c) reveals that the maximum differences in the whole range of the worktable at the same time point are 12.87, 9.79, and 9.11 μm in the X, Y, and Z directions, respectively.

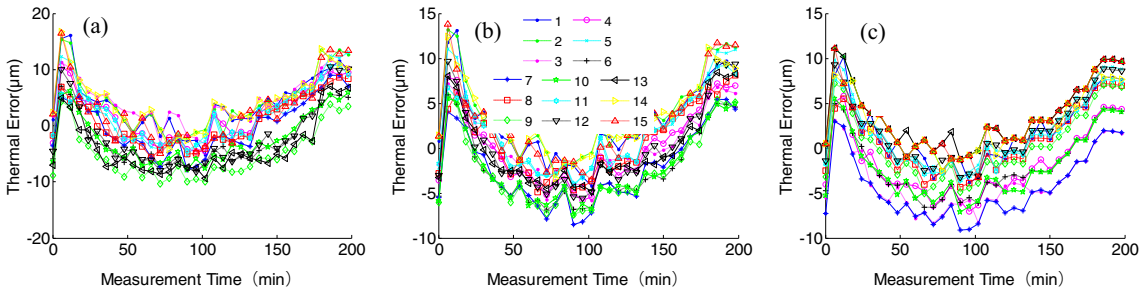

Fig. 10 Thermal errors in the (a) X, (b) Y, and (c) Z directions of 15 points by the single-point method

From a comparison of Figs. 9 and 10, we conclude that both compensation methods can reduce the thermal errors of the whole worktable. The thermal error differences of the whole worktable under the 2D error map method are substantially lower than those under the single-point method. Thus, the compensation effect of the 2D error map method is better than that of the conventional single-point method for the whole worktable.

5 Conclusions

1. In this paper, the thermal errors in three directions of 15 positions on a worktable are measured by batches of idling experiments on a Leaderway-V450 CNC machine tool. The measurement results show that differences in thermal errors exist between different positions on the worktable. The differences reach 5 μm in the X and Y directions and 11 μm in the Z direction. The results prove that the compensation effect of the conventional single-point thermal error model is affected for the whole range of the worktable. Therefore, the 2D thermal error map compensation method for the whole worktable is proposed, and 2D error map models are established.
2. The prediction effect of the 2D thermal error models for the whole worktable is compared with that of the conventional single-point thermal error model. The comparison results reveal that the standard deviations of the prediction in the X, Y, and Z directions are improved by 1.21 μm (27.9%), 2.37 μm (44.0%), and 2.26 μm (48%), respectively. The algorithm of the 2D thermal error map compensation is embedded into the compensator. Along with the real-time temperature values of the sensitive points and the coordinate value of the machine tool for calculating the thermal error compensation value of the position, the origin offset function of the CNC system is adopted to realize the online compensation of the whole worktable.
3. The significant reduction of the influence of the thermal error differences on the compensation effect of the whole worktable under the proposed compensation method is the key point in this paper. Thus, the single-point robust modeling algorithm is not studied, and experiments K2 to K7 involve the same experimental parameters.

Funding information This work is supported by the Key Project of the National Natural Science Fund of China (grant No. 51490660/51490661) and the National Natural Science Foundation of China (grant No. 51175142/E051102).

References

1. Mayr J, Jedrzejewski J, Uhlmann E, Donmez A, Knapp W, Hartig F, Wendt K, Moriwaki T, Shore P, Schmitt R, Brecher C, Wurz T, Wegener K (2012) Thermal issues in machine tools. CIRP Ann Manuf Technol 61(2):771–791
2. Weck M, McKeown P, Bonse R, Herbst U (1995) Reduction and compensation of thermal errors in machine tools. CIRP Ann Manuf Technol 44(2):589–598
3. Bryan JB (1990) International status of thermal error research. Ann CIRP 39(2):645–656
4. Aronson RB (1996) War against thermal expansion. Manuf Eng 116(6):45–50
5. Ramesh R, Mannan MA, Poo AN (2000) Error compensation in machine tools—a review part II: thermal errors. Int J Mach Tool Manu 40(9):1257–1284
6. Yang J, Yuan J, Ni J (1999) Thermal error mode analysis and robust modeling for error compensation on a CNC turning center. Int J Mach Tool Manu 39(9):1367–1381
7. Miao E, Gong Y, Niu P, Ji C, Chen H (2013) Robustness of thermal error compensation modeling models of CNC machine tools. Int J Adv Manuf Technol 69(9):2593–2603
8. IS0 230-3:2001 (2001) Test code for machine tools—part 3:determination of thermal effects. TC 39, Switzerland
9. Abdulshahed AM, Longstaff AP, Fletcher S, Myers A (2014) Thermal error modelling of machine tools based on ANFIS with fuzzy c-means clustering using a thermal imaging camera. Appl Math Model 39(7):1837–1852
10. Lee JH, Yang SH (2002) Statistical optimization and assessment of a thermal error model for CNC machine tools. Int J Mach Tool Manu 42(1):147–155
11. Miao EM, Liu Y, Liu H, Gao Z, Li W (2015) Study on the effects of changes in temperature-sensitive points on thermal error compensation model for CNC machine tool. Int J Mach Tool Manu 97:50–59
12. En-ming M, Ya-yun G, Lian-chun D, Ji-chao M (2014) Temperature-sensitive point selection of thermal error model of CNC machining center. Int J Adv Manuf Technol 74(5–8):681–691
13. Liu H, Miao EM, Wei XY, Zhuang XD (2017) Robust modeling method for thermal error of CNC machine tools based on ridge regression algorithm. Int J Mach Tool Manu 113:35–48
14. Zhang T, Ye W, Shan Y (2016) Application of sliced inverse regression with fuzzy clustering for thermal error modeling of CNC machine tool. Int J Adv Manuf Technol 85(9–12):2761–2771
15. Liu Q, Yan J, Pham DT, Zhou Z, Xu W, Wei Q, Ji C (2016) Identification and optimal selection of temperature-sensitive measuring points of thermal error compensation on a heavy-duty machine tool. Int J Adv Manuf Technol 85(1–4):345–353
16. Zou H, Wang B (2017) Thermal effect on the dynamic error of a high-precision worktable. Arch Civ Mech Eng 17(2):336–343
17. Zhang C (2015) Model of thermal error compensation of large size worktable for machine tools based on piecewise fitting. J Mech Eng 51(3):45–50
18. Ibaraki S, Blaser P, Shimoike M, Takayama N, Nakaminami M, Ido Y (2016) Measurement of thermal influence on a two-dimensional motion trajectory using a tracking interferometer. CIRP Ann Manuf Technol 65(1):483–486

19. Li ET, Zhang GX, Zeng H (2009) Algorithm of surface fitting research based on least-squares methods. J Hangzhou Dianzi Univ
20. Cui GW, Lu J, Gu YF, Gao D, Wang HC, Li CC (2011) Research on real-time synthetic error compensation principle for CNC machine tool. Adv Mater Res 314-316:2454–2457
21. Luo YZ, Gong XY (2004) An algorithm based on bicubic B-spline surface interpolation for free surface design[J]. Spat Struct 10(2): 30–34. (in Chinese)
22. Risa NA (1995) Cubic B-spline interpolation surface and its realization. Mini Micro Syst 03:23–28